Am J Cancer Res 2025;15(4):1597-1613
www.ajcr.us /ISSN:2156-6976/ajcr0160720

Original Article

LncRNA XIST enhances gastric cancer cell function by regulating STAT3/PD-L1 axis as a competing endogenous RNA for miR-124

Gaowa Sharen[1,2], Haoyu Meng[3,4], Lei Zhang[5], Kejian Liu[5], Yu Wang[5], Defang Zhao[5]

[1]Department of Pathology, The Affiliated Hospital of Inner Mongolia Medical University, Hohhot, Inner Mongolia, P. R. China; [2]Department of Pathological Anatomy, College of Basic Medicine of Inner Mongolia Medical University, Hohhot, Inner Mongolia, P. R. China; [3]The Second Affiliated Hospital of Inner Mongolia Medical University, Hohhot, Inner Mongolia, P. R. China; [4]Inner Mongolia Baogang Hospital, Baotou, Inner Mongolia, P. R. China; [5]Department of General Surgery, The Affiliated Hospital of Inner Mongolia Medical University, Hohhot, Inner Mongolia, P. R. China

Received September 24, 2024; Accepted January 2, 2025; Epub April 15, 2025; Published April 30, 2025

Abstract: Objective: To investigate the role and underlying mechanisms of the long non-coding RNA (lncRNA) X inactive-specific transcript (XIST) in gastric cancer (GC). Methods: Real-time quantitative PCR (RT-qPCR), CCK-8, colony formation, flow cytometry, Transwell, and scratch assays were used to evaluate the biological effects of XIST and miR-124 in GC cells. Bioinformatics analysis and dual-luciferase reporter (DLR) assays identified interactions between XIST, miR-124, and STAT3. Western blotting and RT-qPCR assessed changes in downstream targets, while a xenograft tumor model evaluated the in vivo effects of XIST knockdown. Results: XIST was significantly upregulated, and miR-124 was downregulated in GC tissues and cell lines, with the strongest effects observed in MGC803 cells. Knockdown of XIST or overexpression of miR-124 suppressed GC cell proliferation, colony formation, migration, invasion, and promoted apoptosis, effects that were reversed by miR-124 inhibitors. Bioinformatics and DLR assays confirmed that XIST directly targeted miR-124 and regulated STAT3 expression. XIST knockdown increased miR-124 levels, reducing STAT3, PD-1, PD-L1, N-cadherin, and MMP9 expression, while elevating E-cadherin levels; these effects were reversed by miR-124 inhibitors. Additionally, sh-STAT3 mitigated the pro-tumorigenic effects of pcDNA-XIST, confirming the regulatory relationship. In vivo, XIST knockdown suppressed tumor growth by increasing miR-124 expression. Conclusion: XIST promotes STAT3 expression by competitively binding to miR-124, thereby promoting GC progression. Targeting the XIST/miR-124/STAT3 axis may represent a potential therapeutic strategy for GC.

Keywords: LncRNA XIST, miR-124, STAT3, PD-1, PD-L1, gastric cancer, therapeutic targets, biomarker, immunotherapy

Introduction

Gastric cancer (GC) is a prevalent malignancy worldwide and ranks as the second leading cause of cancer-related mortality, primarily due to late-stage diagnosis in many patients [1, 2]. While chemotherapy remains a cornerstone of GC treatment, its survival benefits are limited, and it is often accompanied by severe side effects. With advancements in cancer molecular biology, understanding the molecular mechanisms underlying GC is crucial for developing targeted therapies.

Long non-coding RNAs (lncRNAs) are critical regulators of various cellular processes, including metabolism, proliferation, and differentiation, primarily through their ability to modulate gene transcription. These molecules have been implicated in the progression of numerous cancers [3, 4]. Among them, the lncRNA X inactive-specific transcript (XIST), a key regulator of X chromosome inactivation, has been found to be dysregulated in several cancers, including non-small cell lung cancer (NSCLC), cervical carcinoma, hepatic carcinoma, and GC [5-7].

https://doi.org/10.62347/JBHH9597

In GC, XIST is significantly upregulated in tumor tissues and plasma, with its overexpression correlating with tumor size and advanced TNM stage. LncRNAs often act as competitive endogenous RNAs (ceRNAs) by binding microRNAs (miRNAs), sequestering them, and thereby modulating downstream gene expression. Among miRNAs, miR-124 is a well-characterized tumor suppressor with documented roles in multiple cancers, including GC [8-10]. Recent evidence suggests that XIST knockdown enhances bladder cancer growth, invasion, and migration by competitively binding to miR-124 and targeting the androgen receptor [11]. However, the specific role of XIST in GC progression, particularly its interaction with miR-124, remains poorly understood.

This study aims to investigate the expression profiles of XIST and miR-124 in GC, as well as their functional impact on cellular processes such as proliferation, apoptosis, invasion, and migration. Additionally, it examines the molecular interactions between these molecules. The findings of this research may provide valuable insights and inform the development of novel therapeutic strategies for GC.

Materials and methods

Patient tissue specimens

Primary GC tissue specimens were obtained from 50 patients who underwent surgical resection between January and December 2021 (male-to-female ratio: 31:19; age range: 47-69 years). Tumor and adjacent non-tumor tissues were independently reviewed and verified by two histopathologists based on established histological diagnostic criteria. Stringent inclusion and exclusion criteria were applied to ensure the appropriate selection of primary GC tissue samples.

Inclusion criteria: (1) Patients with a confirmed diagnosis of primary GC based on histopathological evidence. (2) Patients who underwent surgical resection. (3) Patients who had not received preoperative chemotherapy or radiotherapy to avoid treatment-induced tissue alterations.

Exclusion criteria: (1) Patients with secondary or metastatic GC. (2) Patients who received any form of treatment before surgery, including chemotherapy or radiotherapy. (3) Patients whose samples were insufficiently representative or inadequate for analysis. (4) Patients with significant comorbidities potentially affecting study outcomes or those unable to provide informed consent.

Informed consent was obtained from all participants after they were thoroughly informed about the study's objectives, procedures, and potential risks. The research protocol, including the specimen collection process, was reviewed and approved by the Clinical Research Ethics Committee of the Affiliated Hospital of Inner Mongolia Medical University, adhering to ethical research standards. The research project listed has been reviewed and approved by the Institutional Animal Care and Use Committee (IACUC), Affiliated Hospital of Inner Mongolia Medical University in line with the welfare and ethical principles of laboratory animals. Here by certify.

Cell culture

The human gastric mucosal epithelial cell line (GES1) and gastric cancer cell lines (MGC803, BGC823, SGC-7901, AGS) were obtained from the Chinese Academy of Sciences Cell Repository. The cells were cultured in RPMI 1640 medium supplemented with 10% heat-inactivated fetal bovine serum, 100 U/mL penicillin, and 100 μg/mL streptomycin. All cultures were maintained at 37°C in a humidified atmosphere with 5% CO_2.

Cell transfection and grouping

Lentiviral short hairpin RNAs (shRNAs) targeting XIST and STAT3 were designed and subcloned into the pLV-H1TetO-GFP-Puro vector, which was subsequently packaged in HEK-293T cells. Viral particles were harvested 72 hours post-transfection and labeled as sh-XIST and sh-STAT3, respectively. The empty vector (sh-Ctrl) was used as the control.

For transfection into GC cell lines, miR-124 mimics, inhibitors, and a negative control (miR-NC) were delivered using Lipofectamine 2000 (Invitrogen, USA). MGC803 cells were grouped into four transfection categories: (1) sh-Ctrl + miR-NC (blank control group), (2) sh-XIST +

Table 1. RT-PCR primer sequences

Genes	Primer sequence (5'-3')
XIST	F: GCA TAA CTC GGC TTA GGG CT
	R: TCC TCT GCC TGA CCT GCT AT
miRNA-124	F: CTC AAC TGG TGT CGT GGA GTC GGC AAT TCA GTT GA
	R: ACA CTC CAG CTG GGT AAG GCA CGC GGT GAA TGC C
STAT3	F: ATT CTG GCT TCC TTC CTG CC
	R: GCT GAG GCA AGG TGG TTT TG
PD-1	F: ATC TGG AAC TGT GGC CAT GG
	R: GGG GAG GGA GAG AGA GAC AG
PD-L1	F: CCA GGG TGC ACT GAG TCA AT
	R: GCT CAG CCA CAA TTC TTG CC
E-cadherin	F: AGC AGA ACT AAC ACA CGG GG
	R: ATA CCG GGG GAC ACT CAT GA
N-cadherin	F: CGT GAA GGT TTG CCA GTG TG
	R: GTC CTG CTC ACC ACC ACT AC
MMP9	F: CCT TGT GCT CTT CCC TGG AG
	R: GGA CCA CAA CTC GTC ATC GT
U6	F: ATA CAG AGA AAG TTA GCA CGG
	R: GGA ATG CTT CAA AGA GTT GTG
GAPDH	F: TCA TTT CCT GGT ATG ACA ACG A
	R: GTC TTA CTC CTT GGA GGC C

miR-NC (sh-XIST group), (3) sh-Ctrl + miR-124 mimics (miR-124 mimics group), and (4) sh-XIST + miR-124 inhibitors. The sequences for sh-XIST were as follows: sh-XIST#1: 5'-GCC TCG GAT ACC TGC TTT AAT-3', sh-XIST#2: 5'-GTT TGC TAG TGT TTG AAT TTA-3', sh-XIST#3: 5'-TGT CAT AGC TTT GCC TAT TAA-3', sh-XIST#4: 5'-TTC ATG GTT CTG TGC AAT AAA-3'. The seqTence of sh-STAT3#1: 5'-TTC AGA CCC GTC AAC AAA TTA-3', sh-STAT3#2: 5'-ATT GAT GCA GTT TGG AAA TAA-3', sh-STAT3#3: 5'-GGG CTT ACC ATT GGG TTT AAA-3', sh-STAT3#4: 5'-GCC CTG TTG TGG CCC ATT AAA-3'.

Quantitative real-time polymerase chain reaction (qRT-PCR)

Total RNA was isolated from cultured cells and flash-frozen tissue samples using Trizol reagent (Life Technologies, USA). RNA purity and concentration were assessed before reverse transcription into complementary DNA using SuperScript® IV reverse transcriptase (Life Technologies). Quantitative PCR was performed using Power SYBR Green PCR Master Mix (Applied Biosystems) on an ABI 7500 Fast Real-Time PCR System, following the manufacturer's protocol. Primer sequences are detailed in **Table 1**.

Western blot

Proteins were extracted from tissue and cell samples using RIPA buffer (Beyotime, China) supplemented with protease inhibitors (Sigma, USA). Protein concentrations were quantified using a BCA protein assay kit. Equal amounts of protein were separated on a 10% SDS-PAGE gel and transferred onto PVDF membranes (Millipore, USA). The membranes were blocked with 5% skim milk for 2 hours and then incubated overnight at 4°C with primary antibodies against STAT3, p-STAT3, PD-1, PD-L1, E-cadherin, N-cadherin, MMP-9, and GAPDH (all from Cell Signaling Technology, USA). Secondary antibodies were applied for 2 hours at room temperature. Protein bands were visualized using an enhanced chemiluminescence reagent and analyzed with the Tanon-3500 automatic digital imaging system (Tanon, China). Protein expression levels were normalized to GAPDH and quantified by comparing the gray values of the target protein bands to those of GAPDH.

CCK-8 analysis

MGC803 cells (1×10^5 cells/well) from each group were seeded into 96-well plates. On days 1, 2, 3, 4, and 5 after seeding, 100 μL of CCK-8 reagent (Dojindo, Japan) was added to each well. Plates were incubated, and the optical density at 450 nm was measured using a BioTek multifunctional microplate reader (BioTek, USA).

Clone formation assay

MGC803 cells in the logarithmic growth phase were treated with 0.25% trypsin to generate a single-cell suspension, which was seeded into 6-well plates at a density of 50 cells per well. Plates were incubated at 37°C with 5% CO_2 for two weeks. Colonies were then fixed, stained with hematoxylin, and counted.

Cell apoptosis analysis

MGC803 cells were harvested and resuspended in binding buffer. The cells were stained with

FITC-conjugated Annexin V and PI using the Annexin V-FITC/PI Apoptosis Detection Kit (Sangon, China) following the manufacturer's instructions. Apoptotic rates were analyzed using a FACS flow cytometer (BD, USA).

Transwell invasion assay

The upper surfaces of Transwell chambers (Corning, USA) were coated with a mixture of DMEM containing 0.5% FBS and Matrigel (Corning, USA) at a 1:5 dilution. The chambers were incubated at 37°C in a 5% CO_2 atmosphere for 4 hours to solidify the coating. MGC803 cells were cultured in medium supplemented with 5% FBS for 24 hours, digested, resuspended in serum-free medium, and seeded into the upper chambers at a density of 3×10^4 cells/well. The lower chambers were filled with medium containing 20% FBS and incubated at 37°C with 5% CO_2 for 72 hours. After incubation, cells on the upper surface of the membrane were removed, while invasive cells on the lower surface were stained, rinsed with PBS, and counted under a microscope (Olympus, Japan). Invasive cells were quantified in five random fields for each group.

Scratch assay

Cell migration was assessed using a scratch assay. MGC803 cells were seeded into 6-well plates. Upon reaching full confluence, a sterile 200 μL pipette tip was used to create a straight scratch in the cell monolayer. Cells were washed three times with PBS to remove debris and cultured in fresh medium under standard conditions (37°C, 5% CO_2). The wound area was photographed at 0 and 36 hours to evaluate the degree of closure.

Dual-luciferase reporter (DLR) gene assay

The predicted wild-type (WT) and mutant (Mut) sequences of the XIST binding site for miR-124 were cloned into pmirGLO vectors (Promega, USA). MGC803 cells were co-transfected with 10 μg of either pmirGLO-XIST-WT or pmirGLO-XIST-Mut and miR-124 mimics or inhibitors (RiboBio, China) using Lipofectamine 2000. Similarly, WT and Mut sequences of the STAT3 binding site for miR-124 were subcloned into the pmirGLO vector and co-transfected under the same conditions. Luciferase activity was measured using the DLR assay system (Promega, USA).

In vivo experiments

Five-week-old male BALB/c nude mice were randomly allocated into four groups: negative control (NC), sh-XIST, miR-124 mimic, and sh-XIST + miR-124 inhibitor (n = 6 per group). The mice were obtained from the Animal Experiment Center of Inner Mongolia Medical University. MGC803 cells transfected with the corresponding vectors were suspended in 0.2 mL of phosphate-buffered saline (PBS) and injected subcutaneously into the peritoneal region of each mouse (5×10^5 cells/mouse). Tumor growth and mouse behavior were monitored daily over a 42-day observation period, with measurements of tumor dimensions taken every five days using calipers. At the study's end, mice were euthanized under anesthesia with intraperitoneal sodium pentobarbital (0.1 mL/kg), followed by cervical dislocation. Subcutaneous tumors were excised for subsequent analysis.

Statistical analysis

Continuous variables are expressed as mean ± standard deviation (mean ± SD). Statistical differences between groups were analyzed using either a t-test or one-way ANOVA, with $P < 0.05$ considered statistically significant. Data analysis and graph generation were performed using GraphPad Prism and SPSS software.

Results

Expression analysis of XIST and miR-124 in GC tissues and cell lines

We analyzed the expression levels of XIST and miR-124 in GC tissues and adjacent non-neoplastic tissues using RT-qPCR. XIST expression was significantly elevated, while miR-124 levels were markedly reduced in GC tissues compared to the adjacent normal tissues, with statistical significance (**Figure 1A** and **1B**). Further analysis revealed that higher XIST expression was associated with poorer tumor differentiation, greater lymph node metastasis, larger tumor size, and advanced clinical stage (all $P < 0.001$). However, no significant correla-

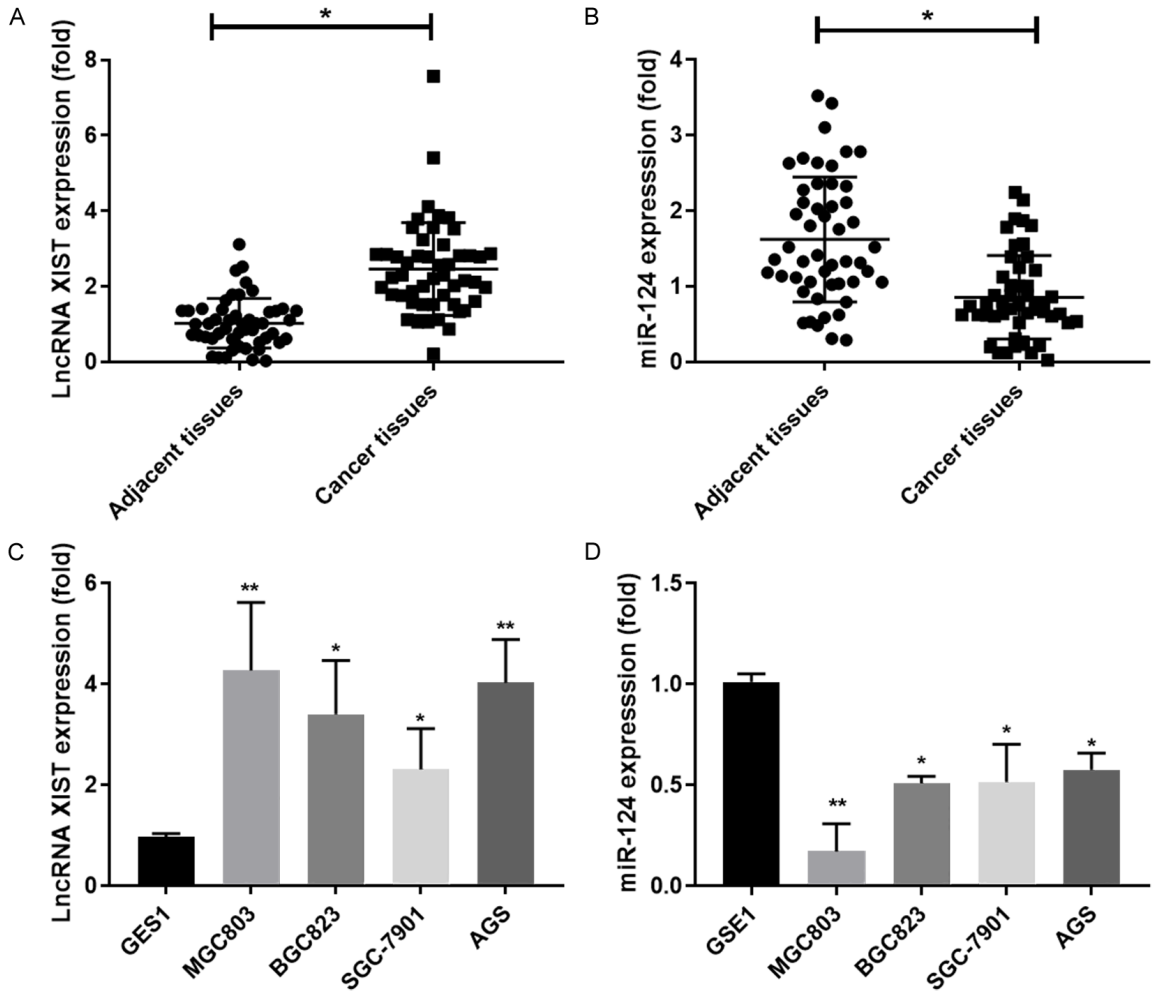

Figure 1. LncRNA XIST and miR-124 in GC tissue specimens and cell strains. A, B. qRT-PCR quantified lncRNA XIST and miR-124 levels in 50 GC tissue specimens compared with adjacent counterparts. C, D. qRT-PCR quantified LncRNA XIST and miR-124 in four GC cell strains (MGC803, BGC823, SGC-7901 and AGS) and human gastric mucosa epithelial cells GSE1. GAPDH was the internal control in this experiment. $^{*}P < 0.05$, $^{**}P < 0.01$.

tion was found with patient age or gender (both P > 0.05, **Table 2**).

We then assessed XIST and miR-124 expression in the human gastric epithelial cell line (GES-1) and four GC cell lines (MGC803, BGC823, SGC-7901, and AGS). RT-qPCR analysis demonstrated a significant upregulation of XIST in all GC cell lines compared to GES-1, with the highest expression in MGC803. Conversely, miR-124 expression was significantly downregulated in the GC cell lines, with the most pronounced reduction in MGC803 (P < 0.05) (**Figure 1C** and **1D**). These results indicate that dysregulation of XIST and miR-124 in GC tissues and cell lines may play a crucial role in disease progression.

Knocking down XIST reduces GC cell growth and clonogenic potential by modulating miR-124

To investigate the regulatory roles of XIST and miR-124 in GC cells, four shRNA constructs targeting XIST were designed. RT-qPCR analysis identified sh-XIST#3 as the most effective construct for XIST knockdown, which was selected for further experiments (**Figure 2A**).

MGC803 cells were transfected with miR-124 mimics or inhibitors, and high transfection efficiency was confirmed via RT-qPCR (**Figure 2B**). Cell proliferation and clonogenic potential were assessed using CCK-8 and colony formation assays, respectively (**Figure 2C** and **2D**).

Table 2. Relationship between lncRNA XIST expression and clinicopathological characteristics of patients with gastric cancer

Clinicopathological characteristics	LncRNA XIST		p
	High expression group n = 37	Low expression group n = 13	
Age			> 0.05
< 55 years	12	4	
≥ 55 years	25	9	
Gender			> 0.05
Male	23	8	
Female	14	5	
Tissue differentiation degree			< 0.001
Low differentiation	30	7	
Highly differentiation	7	6	
Tumor diameter			< 0.001
< 3 cm	11	6	
≥ 3 cm	26	7	
TNM stage			< 0.001
I stage	8	6	
II stage	10	5	
III stage	19	2	
Lymph node metastasis			< 0.001
Yes	32	5	
No	5	8	

Knockdown of XIST (sh-XIST) or overexpression of miR-124 via mimics significantly suppressed MGC803 cell proliferation and colony formation compared to the control group ($P < 0.05$). Moreover, the inhibitory effects of sh-XIST on proliferation and clonogenic capacity were notably reversed upon co-treatment with miR-124 inhibitors compared to the sh-XIST group alone ($P < 0.05$).

Knocking down XIST promotes GC cell apoptosis via modulating miR-124

To evaluate the impact of XIST on apoptosis in MGC803 cells, flow cytometry analysis was performed (**Figure 3**). The apoptotic rates significantly increased in the sh-XIST and miR-124 mimic groups compared to the blank control group ($P < 0.05$). However, co-treatment with sh-XIST and miR-124 inhibitors substantially reduced apoptosis levels compared to the sh-XIST group alone ($P < 0.05$).

Knocking down XIST reduces GC cell invasion and migration via modulating miR-124

Using Transwell and scratch wound healing assays, we assessed the effects of XIST and miR-124 on the invasion and migration capabilities of GC cells (**Figure 4**). The results demonstrated that both invasive and migratory activities were significantly suppressed in the sh-XIST and miR-124 mimics groups compared to the blank control group ($P < 0.05$). Furthermore, co-transfection with sh-XIST and miR-124 inhibitors partially reversed the suppressive effects of sh-XIST on cell invasion and migration ($P < 0.05$).

Targeting the XIST/miR-124/STAT3 axis

The interaction between lncRNAs and miRNAs in cancer biology is well-established. Using Starbase 2.0, we identified a complementary binding site between XIST and miR-124, suggesting that XIST may regulate miR-124. This hypothesis was confirmed by a dual-luciferase reporter assay in MGC803 cells. Co-transfection of miR-124 mimics with the wild-type XIST reporter significantly reduced luciferase activity, whereas the mutant XIST reporter showed no significant changes (**Figure 5A**).

RT-qPCR further validated that XIST knockdown (sh-XIST) increased miR-124 expression in MGC803 cells (**Figure 5B**). Additionally, dual-

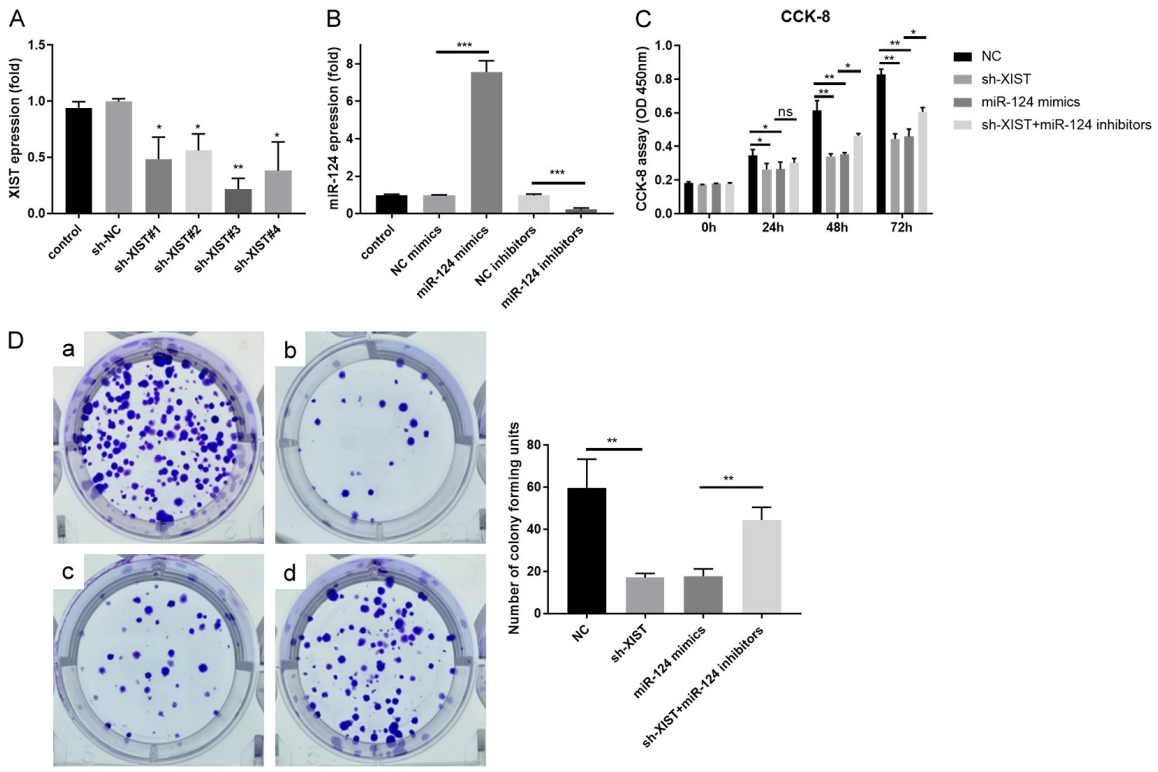

Figure 2. Knocking down lncRNA XIST reduces GC cell proliferation and cloning via regulating miR-124. A. RT-qPCR detection of XIST expression in GC cells, which transfected with sh-XIST#1, sh-XIST#2, sh-XIST#3, sh-XIST#4. B. RT-qPCR detection of miR-124 expression in GC cells, which transfected with miR-124 mimic and miR-124 inhibitor. C. CCK8 assay determines cell proliferation in GC cells at 0 h, 24 h, 48 h, 72 h. D. Colony formation assay determines cell colony in GC cells. a: NC group, b: sh-XIST group, c: miR-124 mimics group, d: sh-XIST + miR-124 inhibitors group. The number of clonal colonies was counted. $^{*}P < 0.05$, $^{**}P < 0.01$.

luciferase assays demonstrated that miR-124 mimics significantly suppressed the activity of the wild-type STAT3 reporter, with no effect on the mutant STAT3 reporter (**Figure 5C** and **5E**).

RT-qPCR and western blot analyses confirmed that sh-XIST or miR-124 mimics decreased STAT3 mRNA and protein levels compared to the controls ($P < 0.05$). The suppression of STAT3 expression by sh-XIST was notably reversed by miR-124 inhibition (**Figure 5D** and **5F**, $P < 0.05$).

XIST regulates expression of STAT3, PD-1, PD-L1, E-cadherin, N-cadherin, and MMP9 in GC cells via targeting miR-124

RT-qPCR and western blot analyses showed that sh-XIST or miR-124 mimics significantly reduced the expression of STAT3, PD-1, PD-L1, N-cadherin, and MMP9 at both transcriptional and protein levels, while increasing E-cadherin expression compared to the control group. However, these effects were partially reversed by co-transfection with sh-XIST and miR-124 inhibitors (**Figure 6** and Supplementary Data).

XIST acts as an oncogene in GC by up-regulating STAT3 expression

To explore whether STAT3 acts downstream of XIST, we analyzed STAT3 expression in GC cell lines. Western blot results showed that STAT3 was significantly upregulated in GC cell lines (MGC803, BGC823, SGC-7901, and AGS) compared to normal gastric mucosal epithelial cells (GES-1) (**Figure 7A**). Among four shRNAs targeting STAT3, sh-STAT3#4 achieved the highest knockdown efficiency and was selected for further experiments (**Figure 7B**). Overexpression of pcDNA-XIST resulted in a > 7-fold increase in XIST expression compared to the control group (**Figure 7C**).

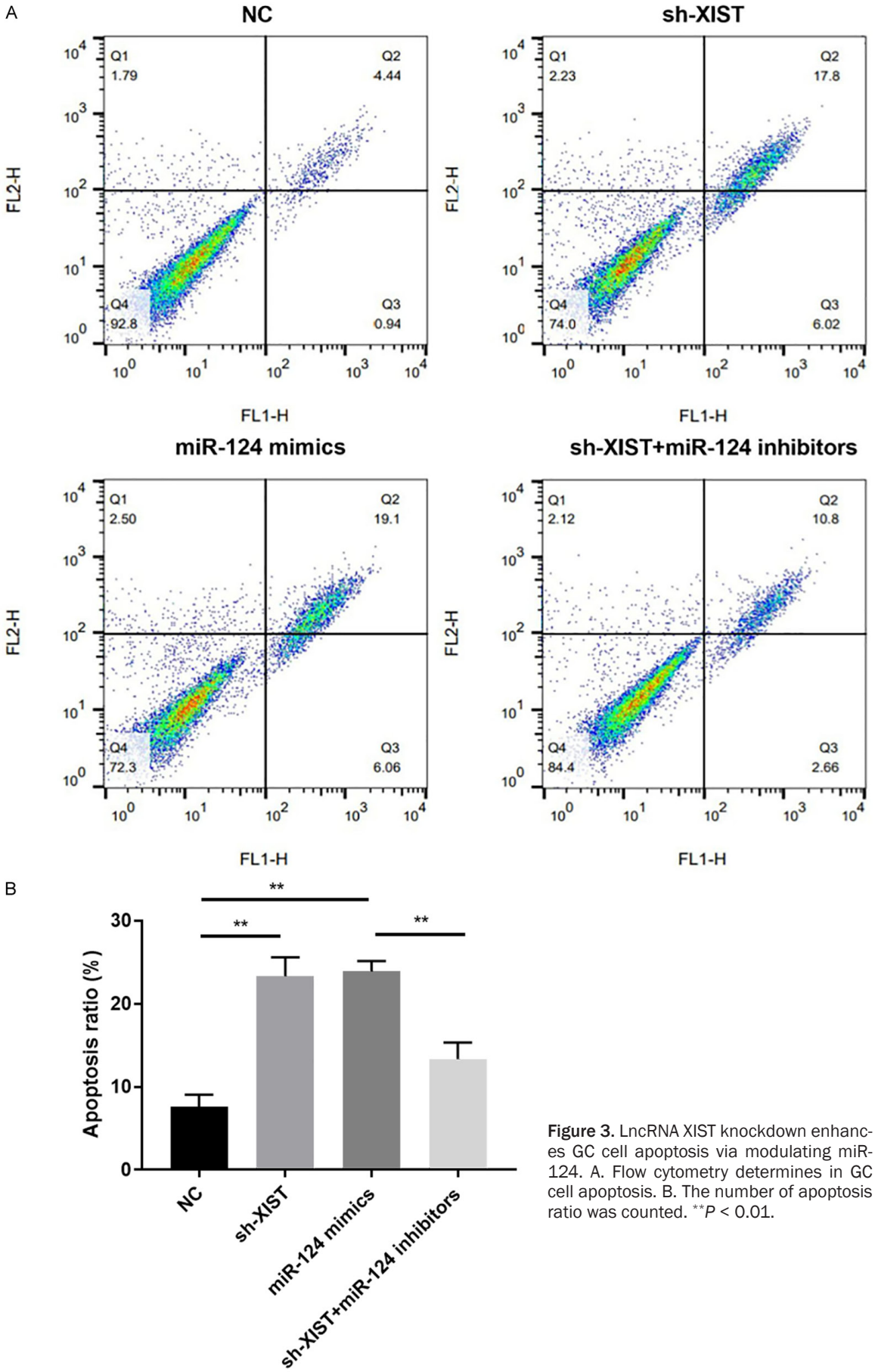

Figure 3. LncRNA XIST knockdown enhances GC cell apoptosis via modulating miR-124. A. Flow cytometry determines in GC cell apoptosis. B. The number of apoptosis ratio was counted. $^{**}P < 0.01$.

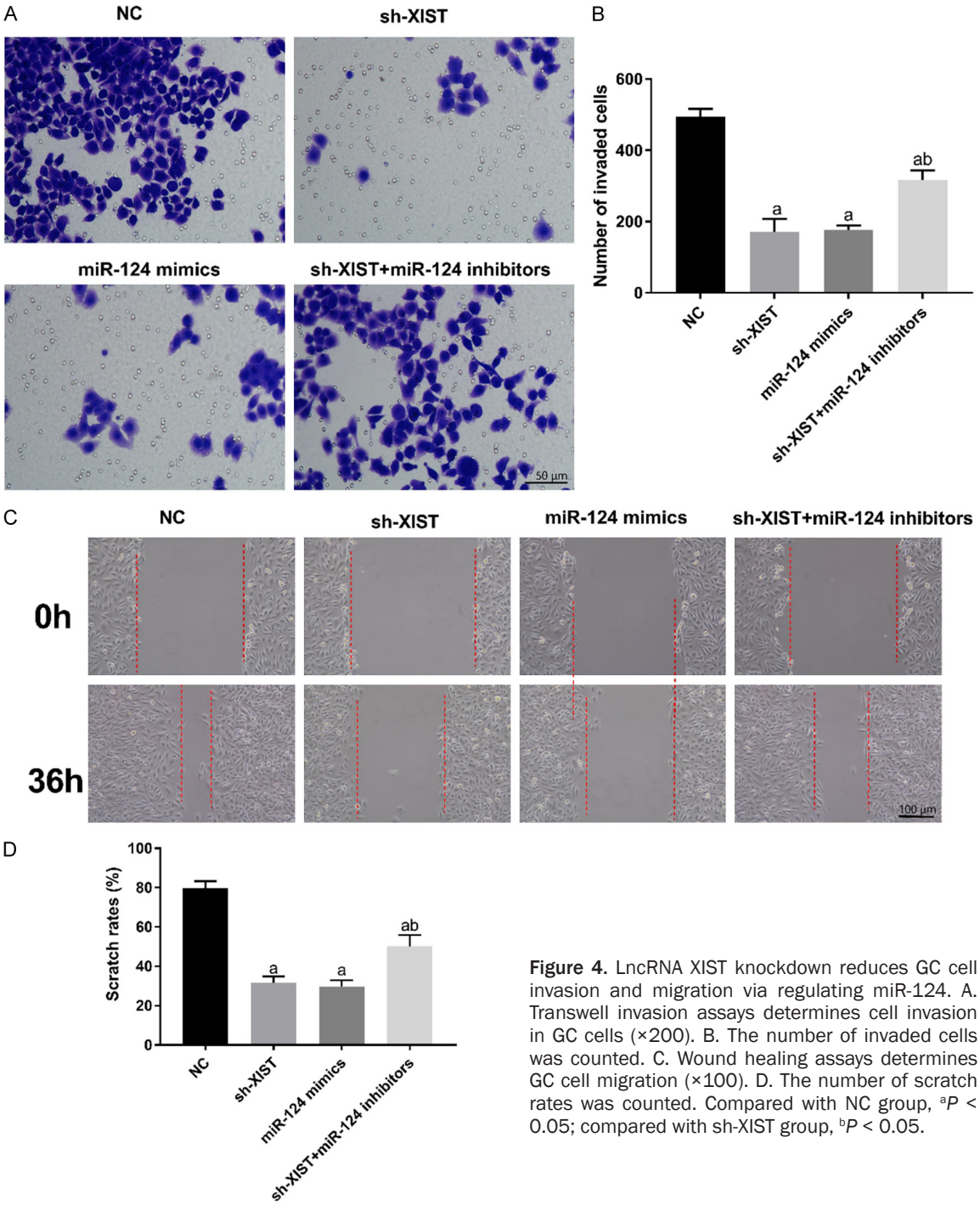

Figure 4. LncRNA XIST knockdown reduces GC cell invasion and migration via regulating miR-124. A. Transwell invasion assays determines cell invasion in GC cells (×200). B. The number of invaded cells was counted. C. Wound healing assays determines GC cell migration (×100). D. The number of scratch rates was counted. Compared with NC group, $^{a}P < 0.05$; compared with sh-XIST group, $^{b}P < 0.05$.

In MGC803 cells, transfection with sh-STAT3 significantly reduced STAT3 expression, while co-transfection with pcDNA-XIST restored STAT3 expression to levels comparable to the control group (**Figure 7D** and **7E**). STAT3 knockdown also decreased the expression of PD-1, PD-L1, N-cadherin, and MMP9 while increasing E-cadherin expression; these effects were reversed by XIST overexpression (**Figure 7E** and **7F**).

Functional assays showed that STAT3 knockdown inhibited cell proliferation (**Figure 7G**), colony formation (**Figure 7H**), invasion (**Figure 7I**), and migration (**Figure 7J**), while promoting apoptosis (**Figure 7K**). Co-transfection with

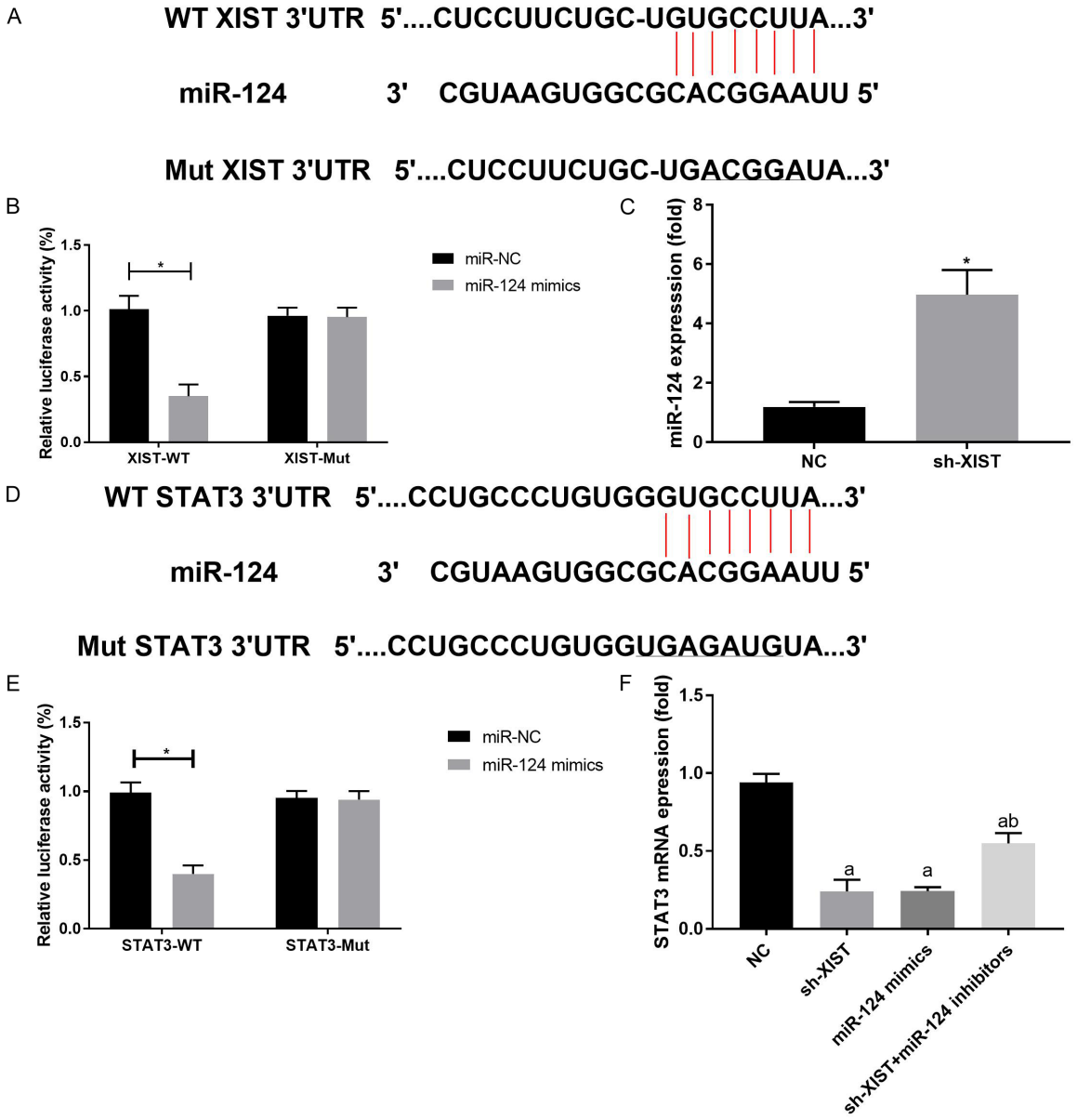

Figure 5. Confirmation of the lncRNA XIST/miR-124/STAT3 axis regulation. A. The potential binding sites for miR-124 on XIST were forecasted using miRcode. B. A luciferase reporter assay was conducted to assess the interaction between lncRNA XIST and miR-124 in GC cells. C. RT-qPCR was utilized to measure the levels of miR-124 in GC cells following transfection with sh-XIST. D. The predicted binding sites for miR-124 on STAT3 were identified using Targetscan 7.2. E. The interaction between STAT3 and miR-124 in GC cells was evaluated using a luciferase reporter assay. F. The levels of STAT3 in GC cells were analyzed after transfection with sh-XIST or treatment with miR-124 mimics or inhibitors. WT, wild type; Mut, mutant; NC, negative control. $^{*}P < 0.05$. Compared with miR-NC or NC group, $^{a}P < 0.05$; compared with sh-XIST group, $^{b}P < 0.05$.

pcDNA-XIST counteracted these effects of sh-STAT3.

Knockdown of XIST inhibits GC xenograft tumor growth by promoting miR-124 expression

To validate our in vitro findings that XIST knockdown inhibits GC progression, we assessed the role of the XIST/miR-124 axis in a xenograft mouse model. MGC803 cells, stably transfected with sh-XIST, miR-124 mimics, or a combination of sh-XIST and miR-124 inhibitors, were subcutaneously injected into athymic mice to evaluate the in vivo effects of this axis on tumor proliferation. Both XIST knockdown and miR-124 overexpression significantly

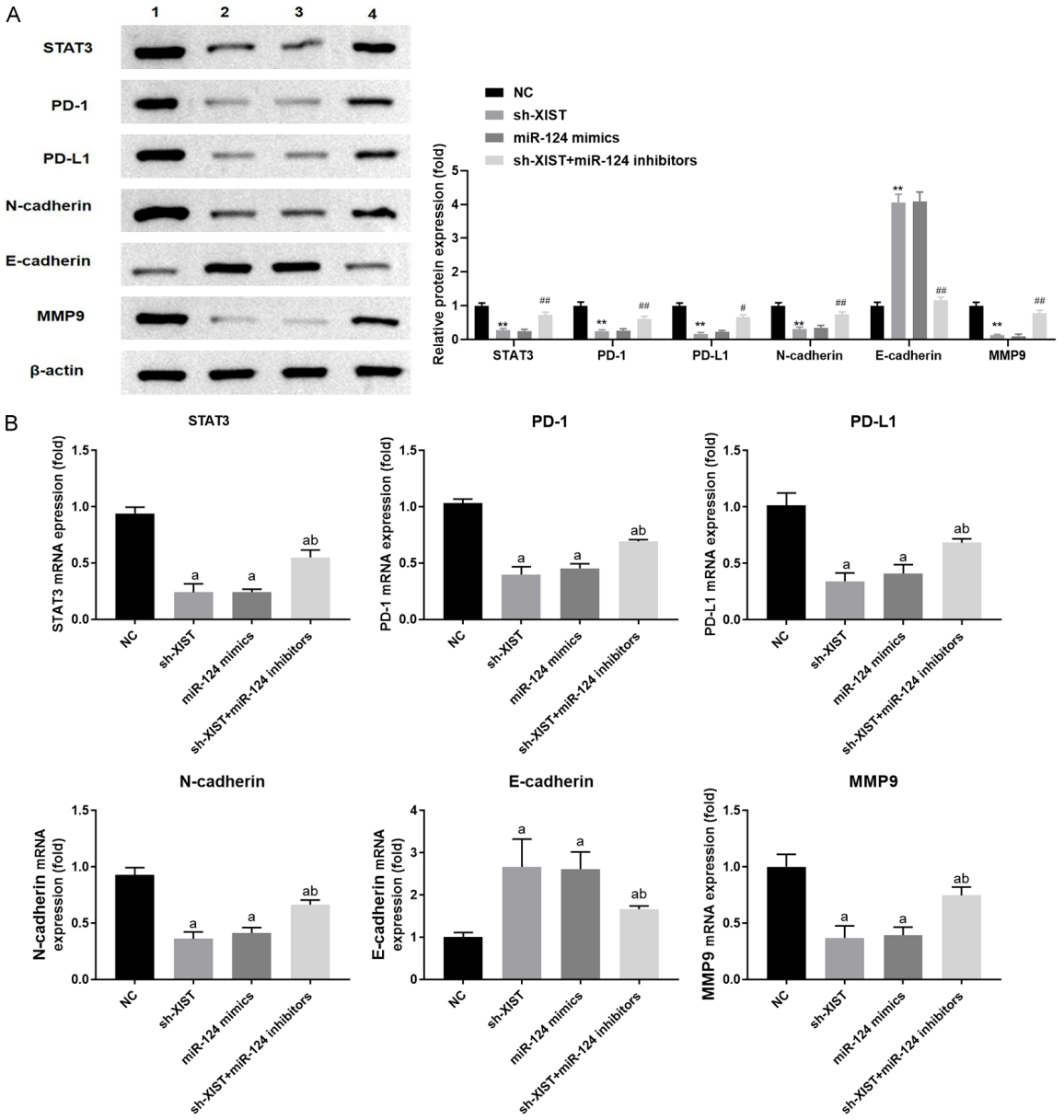

Figure 6. LncRNA XIST affects STAT3, PD-1, PD-L1, E-cadherin, N-cadherin, and MMP9 levels in GC cells via targeting miR-124. A. Western blot quantified STAT3, PD-1, PD-L1, E-cadherin, N-cadherin, and MMP9 levels. 1: NC group, 2: sh-XIST group, 3: miR-124 mimics group, 4: sh-XIST + miR-124 inhibitors group. B. RT-qPCR analyzed PD-1, PD-L1, E-cadherin, N-cadherin, and MMP9 mRNA in GC cells transfected with sh-XIST or miR-124 mimics or inhibitors. Compared with NC group, $^{**}P < 0.01$; compared with sh-XIST group, $^{\#}P < 0.05$, $^{\#\#}P < 0.01$.

reduced tumor volume and weight compared to the NC group. Rescue experiments demonstrated that miR-124 inhibition partially reversed the tumor-suppressive effects of XIST knockdown (**Figure 8A-C**).

Further analysis revealed that XIST knockdown or miR-124 overexpression decreased the expression of XIST, STAT3, and PD-L1 while increasing miR-124 levels. However, co-transfection with miR-124 inhibitors counteracted these changes, as shown in **Figure 8D**. These results are consistent with our in vitro findings and confirm that XIST knockdown suppresses GC tumor growth by enhancing miR-124 expression.

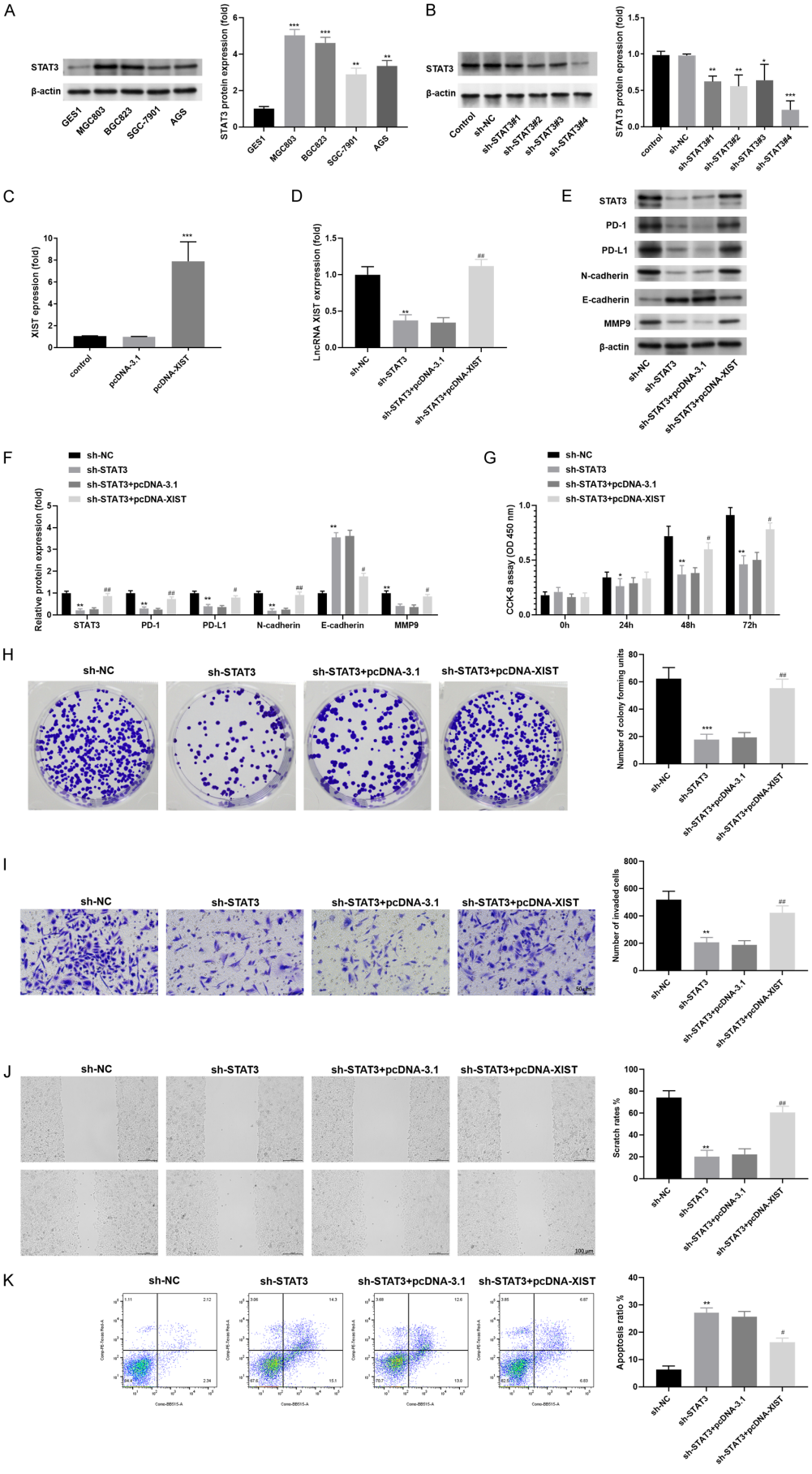
A
STAT3
β-actin
GES1
MGC803
BGC823
SGC-7901
AGS
STAT3 protein expression (fold)
B
STAT3
β-actin
Control
sh-NC
sh-STAT3#1
sh-STAT3#2
sh-STAT3#3
sh-STAT3#4
STAT3 protein epression (fold)
control
sh-NC
sh-STAT3#1
sh-STAT3#2
sh-STAT3#3
sh-STAT3#4
C
XIST epression (fold)
control
pcDNA-3.1
pcDNA-XIST
D
LncRNA XIST exrpression (fold)
sh-NC
sh-STAT3
sh-STAT3+pcDNA-3.1
sh-STAT3+pcDNA-XIST
E
STAT3
PD-1
PD-L1
N-cadherin
E-cadherin
MMP9
β-actin
sh-NC
sh-STAT3
sh-STAT3+pcDNA-3.1
sh-STAT3+pcDNA-XIST
F
sh-NC
sh-STAT3
sh-STAT3+pcDNA-3.1
sh-STAT3+pcDNA-XIST
Relative protein expression (fold)
STAT3
PD-1
PD-L1
N-cadherin
E-cadherin
MMP9
G
sh-NC
sh-STAT3
sh-STAT3+pcDNA-3.1
sh-STAT3+pcDNA-XIST
CCK-8 assay (OD 450 nm)
0h
24h
48h
72h
H
sh-NC
sh-STAT3
sh-STAT3+pcDNA-3.1
sh-STAT3+pcDNA-XIST
Number of colony forming units
I
sh-NC
sh-STAT3
sh-STAT3+pcDNA-3.1
sh-STAT3+pcDNA-XIST
Number of invaded cells
J
sh-NC
sh-STAT3
sh-STAT3+pcDNA-3.1
sh-STAT3+pcDNA-XIST
Scratch rates %
K
sh-NC
sh-STAT3
sh-STAT3+pcDNA-3.1
sh-STAT3+pcDNA-XIST
Apoptosis ratio %

Figure 7. XIST plays an oncogenic role in GC by up-regulating STAT3 expression. A. Western blot quantified STAT3 in four GC cell strains (MGC803, BGC823, SGC-7901 and AGS) and normal gastric mucosal epithelia GES1. β-actin was the internal control in this experiment. $^{*}P < 0.05$, $^{**}P < 0.01$. B. Western blot detection of STAT3 expression in GC cells, which transfected with sh-STAT3#1, sh-STAT3#2, sh-STAT3#3, sh-STAT3#4. C. RT-qPCR detection of XIST expression in GC cells, which transfected with pcDNA-XIST. D. qRT-PCR quantified LncRNA XIST in MGC803 cells, which transfected with sh-NC, sh-STAT3, sh-STAT3 + pcDNA-3.1, sh-STAT3 + pcDNA-XIST. E, F. Western blot quantified protein levels of STAT3, PD-1, PD-L1, E-cadherin, N-cadherin, and MMP9 in MGC803 cells, which transfected with sh-NC, sh-STAT3, sh-STAT3 + pcDNA-3.1, sh-STAT3 + pcDNA-XIST. G. CCK8 assay determines cell proliferation in MGC803 cells at 0 h, 24 h, 48 h, 72 h. H. Colony formation assay determines cell colony in GC cells. I. Transwell invasion assays determines cell invasion in GC cells (×200). J. Wound healing assays determines GC cell migration (×100). K. Flow cytometry determines in GC cell apoptosis, and the number of apoptosis ratio was counted. $^{**}P < 0.01$ compared with sh-NC group. $^{\#\#}P < 0.01$ compared with sh-STAT3 + pcDNA-3.1 group.

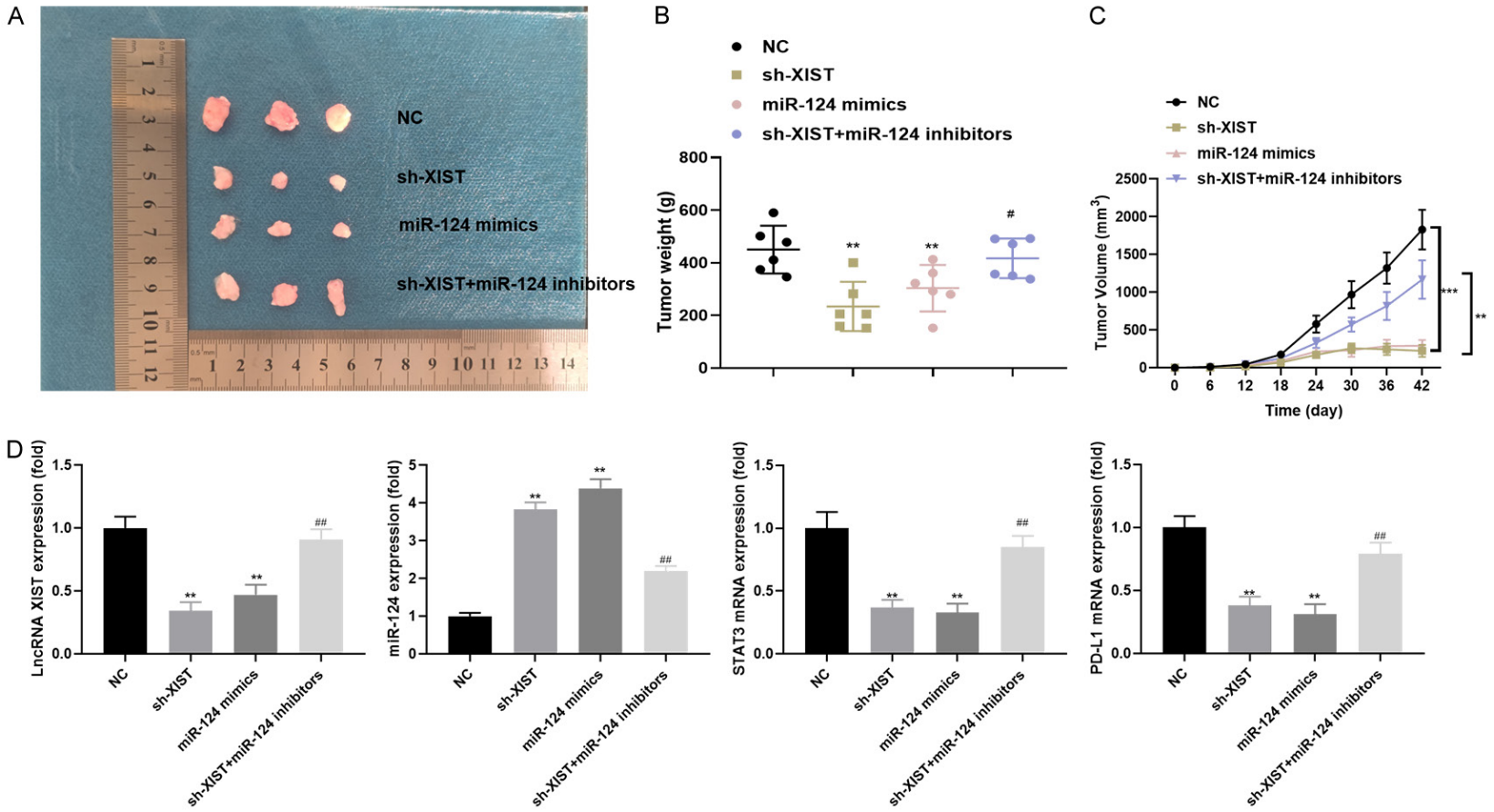

Figure 8. Knockdown of XIST inhibits GC xenograft tumor growth by promoting miR-124 expression. A. Depictions of tumors harvested from each experimental cohort. B. Quantification of tumor volumes across the different groups. C. Measurement of tumor weights in each group. D. RT-qPCR analysis of XIST, miR-124, STAT3 mRNA, and PD-L1 mRNA levels in tumors from each group. $^{**}P < 0.01$, $^{***}P < 0.001$ compared with NC group. $^{\#}P < 0.05$, $^{\#\#}P < 0.01$ compared with sh-XIST group.

Discussion

XIST overexpression has been implicated in various digestive tract cancers, including pancreatic, esophageal, colorectal, and GC [12, 13]. As a ceRNA, XIST regulates miRNA-mRNA networks, influencing tumor behaviors such as proliferation, apoptosis, invasion, and migration [14]. Our study confirmed that XIST is highly expressed, while miR-124 is downregulated in GC tissues and cell lines, consistent with prior research. These findings highlight the critical roles of XIST and miR-124 in GC progression. Xu et al. [15] demonstrated that knocking down XIST promotes apoptosis and enhances cytotoxicity in NSCLC cells. Similarly, Li et al. [16] reported that silencing XIST in glioblastoma affects the sponge-adsorbed miR-448, thereby regulating ROCK1 and ultimately inhibiting tumor cell proliferation, migration, and invasion. In our study, knockdown of XIST using lentiviral sh-XIST suppressed GC cell proliferation, colony formation, invasion, and migration while promoting apoptosis, indicating its tumor-suppressive potential. Similarly, miR-124 mimics significantly reduced GC cell proliferation and invasiveness while enhancing apoptosis. miR-124, a well-established tumor suppressor, is often transcriptionally silenced in various cancers. For instance, Hu et al. [17] demonstrated that miR-124 suppresses GC cell growth and invasion by targeting ROCK1. Additionally, XIST has been identified as an oncogenic factor that regulates miR-124 and miR-140 to promote cyclin expression and pancreatic cancer cell growth [18]. Consistent with this, our study found that XIST knockdown-induced tumor suppression was significantly attenuated by miR-124 inhibitors, suggesting that XIST mediates its effects on GC cells through miR-124.

Bioinformatics analyses identified potential binding sites between XIST and miR-124, which were experimentally confirmed using a dual-luciferase reporter assay. This demonstrated a direct interaction, establishing miR-124 as a target of XIST. As a ceRNA, XIST plays a crucial role in maintaining intracellular gene network stability by engaging in the ceRNA-miRNA-mRNA regulatory axis. Dysregulation of this network is associated with various diseases, including cancer. For instance, Ma et al. [19] reported that XIST sponges miR-497 to regulate MACC1 expression, affecting GC cell growth and invasion. Similarly, our findings revealed that both XIST knockdown and miR-124 overexpression significantly suppressed STAT3 expression. Additionally, miR-124 inhibitors reversed the inhibitory effects of XIST knockdown on STAT3 expression, indicating that XIST modulates STAT3 in GC cells by targeting miR-124.

STAT3, a key factor in the JAK-STAT signaling pathway, plays a critical role in tumor malignancy. The XIST/miR-124 axis may modulate GC cell behavior by regulating STAT3 expression. Qi et al. [20] showed that miR-124 inhibits STAT3 signaling in tumor cells from postoperative NSCLC patients, preventing disease progression. Similarly, Pang et al. [21] reported that miR-124 enhances the radiosensitivity of breast cancer cells by targeting STAT3. In this study, bioinformatics predictions and DLR assays confirmed STAT3 as a direct target of miR-124. Together, these results suggest that XIST regulates STAT3 expression by sequestering miR-124, thereby influencing GC cell biology.

PD-1 and PD-L1 are critical immunosuppressive molecules, overexpressed in various malignancies, and associated with resistance to tumor immunotherapy and poor prognosis [22-24]. The regulation of the PD-1/PD-L1 axis is complex, involving multiple pathways, such as JAK/STAT3, MAPK, and PI3K/Akt [25]. STAT3 acts as an upstream regulator of PD-1/PD-L1 and is crucial for tumor immune regulation. For example, activation of the PD-1 pathway enables immune evasion in head and neck carcinoma cells [26], and STAT3 can bind to the PD-L1 promoter region, facilitating immune escape in cytotoxic NK/T-cell lymphomas [27]. Ashrafizadeh et al. [28] suggested that lncRNAs and miRNAs serve as upstream regulators of the PD-1/PD-L1 axis, crucial for tumor immunomodulation by influencing transcription factors like STAT, PI3K, and Akt. In GC, miR-375 has been shown to inhibit PD-L1 expression by targeting the JAK2/STAT3 axis [29]. Our study demonstrated that XIST knockdown and miR-124 overexpression not only downregulated STAT3 expression but also suppressed PD-1/PD-L1 levels, suggesting that XIST interacts with miR-124 in GC cells and

modulates PD-1/PD-L1 expression through STAT3.

Additionally, XIST was found to regulate the expression of epithelial-mesenchymal transition (EMT)-associated markers, including N-cadherin, E-cadherin, and MMP9, in GC cells via the miR-124/STAT3 axis. Consequently, sh-XIST inhibited EMT in GC cells, suggesting that XIST may influence GC cell behavior by modulating the miR-124/STAT3 axis and impacting the EMT process.

Despite providing valuable insights into the roles of XIST and miR-124 in GC, several limitations should be considered. First, the small sample size may limit the generalizability of the findings. Second, although we identified the XIST/miR-124/STAT3 axis as a regulatory mechanism in GC, the precise molecular interactions and signaling pathways require further exploration. Third, the impact of other genetic and environmental factors on the observed effects of XIST and miR-124 was not investigated. Despite these limitations, our findings lay the foundation for future research and clinical applications. The identification of the XIST/miR-124/STAT3 axis as a critical pathway in GC progression suggests that targeting this axis could offer a promising therapeutic strategy. Future studies should focus on elucidating the detailed molecular mechanisms underlying XIST's regulation of miR-124 and STAT3 in GC, their impact on cellular behavior and EMT, and their potential roles in immunotherapy. Moreover, the development of combination therapies and biomarkers for diagnosis and treatment monitoring should be explored.

In conclusion, XIST is highly expressed in GC, and its knockdown upregulates miR-124 expression, inhibiting GC cell proliferation, clonogenicity, invasion, and migration, while promoting apoptosis. Furthermore, XIST regulates PD-1/PD-L1 expression through STAT3. The XIST/miR-124/STAT3 axis provides valuable insights into GC progression at the molecular level and represents a potential novel therapeutic target. This study highlights the significance of the XIST/miR-124/STAT3 axis in GC and lays the groundwork for future research and therapeutic development. A deeper understanding of these molecular interactions may lead to novel strategies for improving GC management.

Acknowledgements

This work was supported by General Project of Inner Mongolia Medical University (YKD2021-MS021).

Written informed consent was obtained from all participants.

Disclosure of conflict of interest

None.

Abbreviations

GC, gastric cancer; DLR, dual-luciferase reporter; N-cad, N-cadherin; lncRNAs, Long non-coding RNAs; XIST, X inactive-specific transcript; NSCLC, non-small cell lung cancer; ceRNAs, competitive endogenous RNAs; WT, wild-type; Mut, mutant; NC, negative control; PBS, phosphate-buffered saline; ANOVA, analysis of variance.

Address correspondence to: Defang Zhao, Department of General Surgery, The Affiliated Hospital of Inner Mongolia Medical University, No. 5 Xinhua Road, Huimin District, Hohhot 010059, Inner Mongolia, P. R. China. Tel: +86-18204893101; E-mail: zhaodf3863@163.com

References

[1] Jafari-Sales A, Shariat A, Baghi HB, Baradaran B and Jafari B. The presence of human papillomavirus and Epstein-Barr virus infection in GC: a systematic study. Oncologie 2022; 24: 413-426.

[2] Liu Y, Jia Y, Zhang B and Liu A. TUG1 indicate unfavorable prognosis of GC for promoting proliferation, migration and multidrug resistance. Oncologie 2021; 23: 61-72.

[3] Yuan X, Dong Z and Shen S. LncRNA GACAT3: a promising biomarker and therapeutic target in human cancers. Front Cell Dev Biol 2022; 10: 785030.

[4] García-Padilla C, Dueñas Á, García-López V, Aránega A, Franco D, Garcia-Martínez V and López-Sánchez C. Molecular mechanisms of lncRNAs in the dependent regulation of cancer and their potential therapeutic use. Int J Mol Sci 2022; 23: 764.

[5] Liu J, Yao L, Zhang M, Jiang J, Yang M and Wang Y. Downregulation of LncRNA-XIST inhibited development of non-small cell lung cancer by activating miR-335/SOD2/ROS signal path-

way mediated pyroptotic cell death. Aging (Albany NY) 2019; 11: 7830-7846.
[6] Zhu H, Zheng T, Yu J, Zhou L and Wang L. LncRNA XIST accelerates cervical cancer progression via upregulating Fus through competitively binding with miR-200a. Biomed Pharmacother 2018; 105: 789-797.
[7] Chen YK and Yen Y. The ambivalent role of lncRNA XIST in carcinogenesis. Stem Cell Rev Rep 2019; 15: 314-323.
[8] Wu Q, Zhong H, Jiao L, Wen Y, Zhou Y, Zhou J, Lu X, Song X and Ying B. MiR-124-3p inhibits the migration and invasion of gastric cancer by targeting ITGB3. Pathol Res Pract 2020; 216: 152762.
[9] Xia J, Wu Z, Yu C, He W, Zheng H, He Y, Jian W, Chen L, Zhang L and Li W. miR-124 inhibits cell proliferation in gastric cancer through down-regulation of SPHK1. J Pathol 2012; 227: 470-480.
[10] Ghafouri-Fard S, Shoorei H, Bahroudi Z, Abak A, Majidpoor J and Taheri M. An update on the role of miR-124 in the pathogenesis of human disorders. Biomed Pharmacother 2021; 135: 111198.
[11] Xiong Y, Wang L, Li Y, Chen M, He W and Qi L. The long non-coding RNA XIST interacted with MiR-124 to modulate bladder cancer growth, invasion and migration by targeting androgen receptor (AR). Cell Physiol Biochem 2017; 43: 405-418.
[12] Brockdorff N, Bowness JS and Wei G. Progress toward understanding chromosome silencing by Xist RNA. Genes Dev 2020; 34: 733-744.
[13] Zhou Q, Hu W, Zhu W, Zhang F, Lin-Lin L, Liu C, Songyang YY, Sun CC and Li D. Long non coding RNA XIST as a prognostic cancer marker - a meta-analysis. Clin Chim Acta 2018; 482: 1-7.
[14] Berenji E, Valipour Motlagh A, Fathi M, Esmaeili M, Izadi T, Rezvanian P, Zanjirband M, Safaeinejad Z and Nasr-Esfahani MH. Discovering therapeutic possibilities for polycystic ovary syndrome by targeting XIST and its associated ceRNA network through the analysis of transcriptome data. Sci Rep 2024; 14: 6180.
[15] Xu X, Zhou X, Chen Z, Gao C, Zhao L and Cui Y. Silencing of lncRNA XIST inhibits non-small cell lung cancer growth and promotes chemosensitivity to cisplatin. Aging (Albany NY) 2020; 12: 4711-4726.
[16] Li HL, Han PH, Pan DQ, Chen G, Lu XH and Li J. LncRNA XIST regulates cell proliferation, migration and invasion of glioblastoma via regulating miR-448 and ROCK1. J Biol Regul Homeost Agents 2020; 34: 2049-2058.
[17] Hu CB, Li QL, Hu JF, Zhang Q, Xie JP and Deng L. miR-124 inhibits growth and invasion of gastric cancer by targeting ROCK1. Asian Pac J Cancer Prev 2014; 15: 6543-6546.
[18] Liang S, Gong X, Zhang G, Huang G, Lu Y and Li Y. The lncRNA XIST interacts with miR-140/miR-124/iASPP axis to promote pancreatic carcinoma growth. Oncotarget 2017; 8: 113701-113718.
[19] Ma L, Zhou Y, Luo X, Gao H, Deng X and Jiang Y. Long non-coding RNA XIST promotes cell growth and invasion through regulating miR-497/MACC1 axis in gastric cancer. Oncotarget 2017; 8: 4125-4135.
[20] Qi MM, Ge F, Chen XJ, Tang C and Ma J. MiR-124 changes the sensitivity of lung cancer cells to cisplatin through targeting STAT3. Eur Rev Med Pharmacol Sci 2019; 23: 5242-5250.
[21] Pang Y, Wu J, Li X, Wang C, Wang M, Liu J and Yang G. NEAT1/miR-124/STAT3 feedback loop promotes breast cancer progression. Int J Oncol 2019; 55: 745-754.
[22] Dosset M, Vargas TR, Lagrange A, Boidot R, Végran F, Roussey A, Chalmin F, Dondaine L, Paul C, Lauret Marie-Joseph E, Martin F, Ryffel B, Borg C, Adotévi O, Ghiringhelli F and Apetoh L. PD-1/PD-L1 pathway: an adaptive immune resistance mechanism to immunogenic chemotherapy in colorectal cancer. Oncoimmunology 2018; 7: e1433981.
[23] Qing Y, Li Q, Ren T, Xia W, Peng Y, Liu GL, Luo H, Yang YX, Dai XY, Zhou SF and Wang D. Upregulation of PD-L1 and APE1 is associated with tumorigenesis and poor prognosis of gastric cancer. Drug Des Devel Ther 2015; 9: 901-909.
[24] Xiao Y, Jiang J, Chen Y, Huang Y and Wei C. PD-1 relevant genes predict the prognosis of breast cancer and their prediction effect in tumor response to immunotherapy. Oncologie 2022; 24: 729-742.
[25] Jiang X, Wang J, Deng X, Xiong F, Ge J, Xiang B, Wu X, Ma J, Zhou M, Li X, Li Y, Li G, Xiong W, Guo C and Zeng Z. Role of the tumor microenvironment in PD-L1/PD-1-mediated tumor immune escape. Mol Cancer 2019; 18: 10.
[26] Jeong JS, Jo U, Choi G, Song H, Cho KJ and Song JS. Comparison of PD-L1 assays in head and neck carcinoma. Pathology 2024; 56: 969-981.
[27] Song TL, Nairismägi ML, Laurensia Y, Lim JQ, Tan J, Li ZM, Pang WL, Kizhakeyil A, Wijaya GC, Huang DC, Nagarajan S, Chia BK, Cheah D, Liu YH, Zhang F, Rao HL, Tang T, Wong EK, Bei JX, Iqbal J, Grigoropoulos NF, Ng SB, Chng WJ, Teh BT, Tan SY, Verma NK, Fan H, Lim ST and Ong CK. Oncogenic activation of the STAT3 pathway drives PD-L1 expression in natural killer/T-cell lymphoma. Blood 2018; 132: 1146-1158.

[28] Ashrafizadeh M, Zarrabi A, Hushmandi K, Zarrin V, Moghadam ER, Zabolian A, Tavakol S, Samarghandian S and Najafi M. PD-1/PD-L1 axis regulation in cancer therapy: the role of long non-coding RNAs and microRNAs. Life Sci 2020; 256: 117899.

[29] Yan XL, Luo QY, Zhou SN, Pan WT, Zhang L, Yang DJ and Qiu MZ. MicroRNA-375 reverses the expression of PD-L1 by inactivating the JAK2/STAT3 signaling pathways in gastric cancer. Clin Res Hepatol Gastroenterol 2021; 45: 101574.